Chapter 6

Effect of Pressure Difference at the Film-Porous Interface on Squeeze-Film Bearing

Contents

6.1 Introduction

6.2 Mathematical Formulation and Solution

6.3 Numerical Calculations and Discussion of Results

6.4 Conclusions

6.5 Figures

6.6 References

6.1 Introduction

It is well known that squeeze phenomenon arise when two lubricated surfaces (plates or discs) approaches each other with a normal velocity (known as squeeze velocity). In this case the fluid layer between these two surfaces is known as squeeze-film. Many authors have studied this phenomenon for different bearing design systems from different viewpoints because of having its numerous applications on lubrication technology. The studies were mainly focused on the improvement of the performances of various bearing characteristics like load-carrying capacity, friction, coefficient of friction, time-height relationship, etc. Various effects on the solid bearing surfaces like porosity, slip velocity, roughnesses, etc. are considered for the study. Moreover, effects of different lubricants like power-law fluid, couple-stress fluid, magnetic fluid (MF), etc. are also considered. The MHD based bearings are also studied. The following are some references related with squeeze-film designs.

Starting with 1970's, Wu [1] in his analysis discussed the problem of squeeze-film behaviour between porous annular discs, when upper disc with a porous facing approaches the lower impermeable disc, considering no-slip boundary condition at the film-porous interface. Sparrow *et. al.* [2] extended the Wu's analysis [1] with the effect of velocity slip on the film-porous interface. Results for load-carrying capacity and time-height relation are discussed. The results show that the insertion of porous layer leads to decrease in load-carrying capacity while it is effective in diminishing the response times. In particular, substantially faster response can be attained by the use of porous materials which accentuate velocity slip. Murti [3] studied squeeze-film behaviour in porous circular discs, where porous facing attached with the upper disc and lower disc is

impermeable, considering Wu's analysis [1]. The modified Reynolds equation is solved in a closed form and expressions for pressure, load-carrying capacity and time of approach for the plates are obtained in terms of Fourier-Bessel series. It is found that due to enhanced value of the permeability parameter, pressure diminishes over the entire disc. However, adverse effect is observed on the load-carrying capacity and time of approach. Gupta and Patel [4] modified the problem discussed in [2] with the effect of axial current induced pinch and shown the improvement in the bearing performances. Gupta *et. al.* [5] analyzed annular squeeze-film between curved upper porous facing plate and lower impermeable flat plate considering the effect of rotation of both the plates. Expressions for pressure and load-carrying capacity are obtained. It is shown that load-carrying capacity decreases when the speed of rotation of the upper plate increased up to certain value of curvature parameter and then reverse trend is observed. It is also shown that load-carrying capacity could be increased without altering the speed of rotation and increasing values of curvature parameter. Prakash and Tiwari [6] studied effect of surface roughness on the squeeze-film between rotating annular discs with arbitrary porous wall thickness with the porous facing attached with the upper disc. An exact solution, valid for arbitrary wall thickness is discussed for the film pressure as well as pressure in the bearing material. Bhat and Deheri [7] discussed effect of MF on the curved squeeze-film between two circular discs, where porous facing is attached with the upper disc while the lower disc is flat impermeable. Expressions for pressure, load-carrying capacity and response time are obtained, and are found to increase with the increasing magnetization parameter. Elsharkawy and Nassar [8] studied hydrodynamic lubrication of three different types of squeeze-film porous bearings (parallel-surface bearing of infinite width,

journal bearings and parallel circular plates bearing), where porous facing is attached with the lower surface. The closed forms of analytical solutions are obtained. It is shown that with the increase of permeability parameter, both pressure and load-carrying capacity decreases in the case of pure squeeze motion. Shah and Bhat [9] studied circular squeeze-film bearing made by curved upper plate with a porous facing and impermeable flat lower plate, considering rotation of both the plates, using MF lubricant. The results show that pressure, load-carrying capacity and response time increases with the increase in curvature of the upper plate as well as magnetization parameter. Shah and Bhat [10] studied combined effect of anisotropic permeability and slip velocity on porous walled squeeze-films between circular plates lubricated with ferrofluid (FF). It is shown that load-carrying capacity and response time decreases with the increasing values of radial permeability parameter while they increase with the increasing values of axial permeability parameter. Walicka *et. al.* [11] investigated inertia effects in a curvilinear squeeze-film bearing lubricated by a power-law fluid. The lower surface is attached with a porous facing. Using the average inertia method the closed form of solution of Reynolds equation is obtained. Shah and Bhat [12] studied squeeze-film between two parallel plates using FF lubricant with the porous facing attached with the upper plate and various bearing characteristics are studied. Shah and Bhat [13] analyzed squeeze-film in an axially undefined journal bearing with anisotropic permeable porous facing and slip velocity considering FF lubricant. Results show that load-carrying capacity and response time increases with the increasing values of eccentricity ratio and anisotropic parameter while they decrease with increasing values of slip parameter or material parameter. Deheri and Patel [14] discussed MF based squeeze-film between porous circular discs

with sealed boundary with the porous facing attached with the upper disc. It is shown that load-carrying capacity increases significantly. Shah and Bhat [15] studied theoretical FF lubricated secant shaped squeeze-film bearing with the consideration of anisotropic permeability, slip velocity, material parameter and rotational inertia. Results show that load-carrying capacity and response time decreases with the increasing values of radial permeability, slip and rotational inertia. However, they increase with the increasing values of axial permeability and material constant. Bujurke *et. al.* [16] discusses surface roughness effects on the squeeze-film behaviour in porous circular discs with couple-stress fluid. The porous facing is attached with the upper disc and the roughness presented at both the discs. Closed form of solution of the stochastic Reynolds equation is obtained in terms of Fourier-Bessel series. It is shown that the present case is more pronounced as compared to classical case. Rajashekar and Kashinath [17] analyzed effect of surface roughness on MHD couple-stress based squeeze-film between a sphere and a porous plane surface. Expressions for pressure, load-carrying capacity and mean squeeze-time are obtained. It is found that load-carrying capacity increases (decreases) for azimuthal (radial) roughness patterns as compared to the smooth case. The response time is also lengthening in both types of roughnesses. With respect to porous parameter, load-carrying capacity decreases whereas squeeze time increases. Shah and Patel [18] discussed impact of various porous structures on the squeeze-film between curved porous circular and flat plates using FF lubricant. Results show that load-carrying capacity increases in the case of globular sphere model of the porous plate. Fathima *et. al.* [19] studied hydromagnetic squeeze-film between parallel anisotropic porous rectangular plates in the presence of transverse magnetic field with couple-stress fluid. The porous

facing is attached with the lower plate. It is found that load-carrying capacity increases. The squeeze-time is also lengthening as compared to non-magnetic case. Shah *et. al.* [20] discusses review with contributions on some porous squeeze-film bearings with FF lubricant. The bearing performances are found to be better using FF as lubricant. Shah and Kataria [21] studied squeeze-film between a sphere and a flat porous plate using FF as lubricant. The results show the better performance of the bearing characteristics.

In all above studies, Reynolds equation is derived or solved either by assuming Morgan-Cameron approximation (that the pressure in the porous region can be replaced by the average pressure with respect to the bearing wall thickness) or by continuity of the pressure at the film-porous interface. However, due to the effect of squeezing, vibration, etc. the pressure at the film-porous interface may not be equal and there may be an existence of pressure difference P (say). The present Chapter derived modified Reynolds equation for squeeze-film bearing made by flat circular porous upper and impermeable lower discs using FF lubricant (whose flow is governed by R.E. Rosensweig model [22]) controlled by oblique variable magnetic field (VMF) without using Morgan-Cameron approximation [3]. The VMF is considered because uniform magnetic field does not enhance bearing performances. Moreover, it is important because of its advantage of generating maximum field at the required active contact zone. In the present analysis the active contact zone is considered at the middle of the lower disc and so the applied magnetic field is chosen to be maximum at that point. Expression for film pressure is obtained in terms of Bessel function by considering the effect of existence of pressure difference (that is without assuming the pressure continuity condition as in [3,19]) at the film-porous interface and studied. The expression for load-carrying capacity is also

obtained and studied. In general, the same approach can be employed to study any other type of squeeze-film bearing geometry.

6.2 Mathematical Formulation and Solution

The schematic diagram of physical configuration of the problem under consideration is shown in Figure 6.1, which consists of two flat circular impermeable discs, each of radius a. The upper disc is attached with a porous facing (now onwards known as porous upper disc) of width H^*. The two discs are separated by initial thickness h_0. This thickness (known as fluid film region or film thickness) is filled with a FF lubricant. As FF is controlled by applied magnetic field, so oblique (to the lower disc) and VMF **H** with magnitude (strength) H of the form [21]

$$H^2 = \frac{Kr^2(a-r)}{a} \tag{6.1}$$

is used for the study, where r is the radial coordinate. Here, K being a quantity chosen to suit the dimensions of both sides of the equation (6.1). Such a magnetic field attains maximum at $r = 2a / 3$ and vanishes at $r = 0$ and $r = a$.

The porous upper disc approaches the impermeable lower one at a constant normal velocity (known as squeeze velocity)

$$\dot{h} = \frac{dh}{dt}, \tag{6.2}$$

where h is film thickness and t is time.

The basic equation governing the pressure distribution p in the film region in r-direction considering R.E. Rosensweig model for FF flow is given by [21]

$$\frac{\partial}{\partial r}\left(p - \frac{1}{2}\mu_0 \bar{\mu} H^2 \right) = \eta \frac{\partial^2 u}{\partial z^2}$$

(6.3)

under the assumption that the flow is steady, laminar and axisymmetric, the fluid is incompressible and possesses constant properties, all the inertia terms neglected and derivatives of velocities across the film predominate. Here, μ_0, $\bar{\mu}$, η, z are free space permeability, magnetic susceptibility, fluid viscosity and axial coordinate, respectively.

Also,

$$\mathbf{q} = (\dot{r}, r\dot{\theta}, \dot{z}) = (u, rv, w),$$

(6.4)

where (r, θ, z) are cylindrical polar coordinates and dot $(\cdot)$ represents derivative with respect to t. So that u, v, w are respectively radial, tangential and axial velocity components of $\mathbf{q}$.

Integrating equation (6.3) twice w.r.t. z and using boundary conditions

$u = 0$ when $z = 0$ and $u = 0$ when $z = h$,

the expression for u can be obtained, which on substituting in the integral form of continuity equation in cylindrical polar coordinates for the film thickness [0, h], yields

$$\frac{1}{r}\frac{\partial}{\partial r}\left[rh^3 \frac{\partial}{\partial r}\left(p - \frac{1}{2}\mu_0 \bar{\mu} H^2 \right) \right] = 12\eta w\big|_{z=h},$$

(6.5)

where $w\big|_{z=0} = 0$ as lower disc is impermeable.

Assuming that the porous matrix is homogeneous and isotropic, flow in the porous region is axisymmetric, velocities are continuous at the interface between film and

porous region and velocity components in the porous region is governed by Darcy's law, equation (6.5) can be written as

$$\frac{1}{r}\frac{\partial}{\partial r}\left[r\frac{\partial}{\partial r}\left(p-\frac{1}{2}\mu_0\bar{\mu}H^2\right)\right]=\frac{12\eta}{h^3}\left[\frac{dh}{dt}-\frac{\phi}{\eta}\frac{\partial}{\partial z}\left(p^*-\frac{1}{2}\mu_0\bar{\mu}H^2\right)_{z=h}\right]$$

(6.6)

with

$$\frac{1}{r}\frac{\partial}{\partial r}\left[r\frac{\partial}{\partial r}\left(p^*-\frac{1}{2}\mu_0\bar{\mu}H^2\right)\right]+\frac{\partial^2}{\partial z^2}\left(p^*-\frac{1}{2}\mu_0\bar{\mu}H^2\right)=0,$$

(6.7)

where ϕ is the permeability of the porous facing and p^* is the pressure in the porous region.

Using equation (6.1), equations (6.6) and (6.7) becomes

$$\frac{1}{r}\frac{\partial}{\partial r}\left(r\frac{\partial p}{\partial r}\right)-\frac{1}{2a}\mu_0\bar{\mu}K(4a-9r)=\frac{12\eta\dot{h}}{h^3}-\frac{12\phi}{h^3}\left(\frac{\partial p^*}{\partial z}\right)_{z=h}$$

(6.8)

and

$$\frac{\partial^2 p^*}{\partial r^2}+\frac{1}{r}\frac{\partial p^*}{\partial r}+\frac{\partial^2 p^*}{\partial z^2}=\frac{1}{2a}\mu_0\bar{\mu}K\left(4a-9r\right),$$

(6.9)

respectively.

Equation (6.8) with equation (6.9) is the required modified Reynolds equation for the present study. This equation includes the effect of FF lubricant which is controlled by oblique VMF of strength given by equation (6.1) in order to make the required active

contact zone in the neighbourhood of $r = 2a/3$. For other active contact zones, suitable form of magnetic field strength (6.1) should be chosen.

The separation of variables solution of equation (6.9) using boundary conditions

$$\left.\frac{\partial p^*}{\partial z}\right|_{z=h+H^*} = 0, \tag{6.10}$$

$$p^*(a,z) = 0, \tag{6.11}$$

$$\left.\frac{\partial p^*}{\partial r}\right|_{r=0} = 0 \tag{6.12}$$

becomes

$$p^*(r,z) = \sum_{n=1}^{\infty} C_n\, e^{\alpha_n z}\left[1 + e^{2\alpha_n (h+H^*)-2\alpha_n z}\right] J_0(\alpha_n r) + \frac{1}{2}\mu_0 \bar{\mu} H^2, \tag{6.13}$$

where condition (6.10) indicates no flow through the impervious boundary at the top of the porous upper disc, condition (6.11) indicates zero ambient pressure at the end a of the porous facing and condition (6.12) indicates axisymmetric pressure distribution in the porous facing. Moreover, C_n are unknown constants, $\alpha_n=(4n-1)\pi/4a$ is the n^{th}-eigenvalue which satisfies $J_0(\alpha_n a)=0$, Bessel function of first kind of order zero.

Using equation (6.13) with boundary conditions

$$\left.\frac{dp}{dr}\right|_{r=0} = 0,$$

(6.14)

$$p(a) = 0,$$

(6.15)

equation (6.8) gives an expression for pressure distribution p in the film region (film pressure distribution) as

$$p = \frac{1}{2}\mu_0\bar{\mu}H^2 + \frac{3\eta}{h^3}(r^2 - a^2)\dot{h} + \frac{12\phi}{h^3}\sum_{n=1}^{\infty}\frac{C_n e^{\alpha_n h}}{\alpha_n}(1 - e^{2\alpha_n H^*})J_0(\alpha_n r),$$

(6.16)

where condition (6.14) indicates axisymmetric pressure distribution in the film region and condition (6.15) indicates zero ambient pressure at the end a of the film region.

Invoking the modified pressure-continuity condition

$$P + p(r) = p^*(r, h)$$

(6.17)

at the film-porous interface, equations (6.13) and (6.16) yields

$$P + \frac{3\eta}{h^3}(r^2 - a^2)\dot{h} = \sum_{n=1}^{\infty} C_n e^{\alpha_n h}\left[(1 + e^{2\alpha_n H^*}) - \frac{12\phi}{h^3}\frac{(1 - e^{2\alpha_n H^*})}{\alpha_n}\right]J_0(\alpha_n r),$$

(6.18)

where pressure difference P at the film-porous interface may be positive or negative depending on whether porous upper disc applying pressure on film region or vice versa. Moreover, in general, P may dependent on porosity, permeability, width of the porous

facing and other porous medium properties as well as shape of the squeeze-film and lubricant used.

The unknown constants C_n occurring in equation (6.18) can now be evaluated by using the orthogonality of the eigenfunction $J_0(\alpha_n r)$ and is obtained as

$$C_n = \frac{\eta \dot{h}}{h^3}\left[-\frac{24}{a\alpha_n^3 J_1(\alpha_n a)} + \frac{2Ph^3}{a\eta\dot{h}\alpha_n J_1(\alpha_n a)}\right] \times \left[e^{\alpha_n h}\left\{(1+e^{2\alpha_n H^*}) - \frac{12\phi}{h^3\alpha_n}(1-e^{2\alpha_n H^*})\right\}\right]^{-1}. \tag{6.19}$$

Defining the dimensionless quantities

$$R = \frac{r}{a}, \quad \bar{h} = \frac{h}{a}, \quad \bar{H} = \frac{H^*}{a}, \quad \psi = \frac{\phi H^*}{h_0^3}, \quad \bar{\alpha}_n = a\alpha_n,$$

$$\bar{P} = \frac{2Ph^3}{\eta a^2 \dot{h}}, \quad \mu^* = \frac{-K\mu_0 \bar{\mu} h^3}{\eta \dot{h}} \tag{6.20}$$

the unknown constants C_n defined in equation (6.19) in dimensionless form becomes

$$\bar{C}_n = \frac{C_n h^3}{\eta \dot{h} a^2} = \left[-\frac{24}{\bar{\alpha}_n^3 J_1(\bar{\alpha}_n)} + \frac{\bar{P}}{\bar{\alpha}_n J_1(\bar{\alpha}_n)}\right]\left[e^{\bar{\alpha}_n \bar{h}}\left\{(1+e^{2\bar{\alpha}_n \bar{H}}) - 12\psi\left(\frac{h_0}{h}\right)^3 \frac{(1-e^{2\bar{\alpha}_n \bar{H}})}{\bar{\alpha}_n \bar{H}}\right\}\right]^{-1}. \tag{6.21}$$

Using $\bar{C}_n$ obtained in equation (6.21) and dimensionless quantities defined in equation (6.20), the dimensionless form of film pressure p (using equation (6.16)) can be obtained as

$$\bar{p} = -\frac{ph^3}{\eta a^2 \dot{h}} = \frac{1}{2}\mu^* R^2(1-R) - 3(R^2-1) - \sum_{n=1}^{\infty} \frac{24}{\bar{\alpha}_n^3} \frac{J_0(\bar{\alpha}_n R)}{J_1(\bar{\alpha}_n)} \left[1 + \frac{\bar{\alpha}_n \bar{H}(e^{2\bar{\alpha}_n \bar{H}} + 1)}{12\psi \left(\frac{h_0}{h} \right)^3 (e^{2\bar{\alpha}_n \bar{H}} - 1)} \right]^{-1} + P_n, \tag{6.22}$$

where

$$P_n = \sum_{n=1}^{\infty} \frac{\bar{P}}{\bar{\alpha}_n} \frac{J_0(\bar{\alpha}_n R)}{J_1(\bar{\alpha}_n)} \left[1 + \frac{\bar{\alpha}_n \bar{H}(e^{2\bar{\alpha}_n \bar{H}} + 1)}{12\psi \left(\frac{h_0}{h} \right)^3 (e^{2\bar{\alpha}_n \bar{H}} - 1)} \right]^{-1}. \tag{6.23}$$

The load-carrying capacity W of the squeeze-film is found by integrating the pressure over the disc surface

$$W = 2\pi \int_0^a pr \ dr.$$

Using equations (6.20) and (6.22), the dimensionless form of load-carrying capacity can be expressed as

$$\bar{W} = \frac{Wh^3}{a^4 \eta \dot{h}} = \frac{\pi}{20}\mu^* + \frac{3\pi}{2} - \sum_{n=1}^{\infty} \frac{48\pi}{\bar{\alpha}_n^4} \left[1 + \frac{\bar{\alpha}_n \bar{H}(e^{2\bar{\alpha}_n \bar{H}} + 1)}{12\psi \left(\frac{h_0}{h} \right)^3 (e^{2\bar{\alpha}_n \bar{H}} - 1)} \right]^{-1} + W_n, \tag{6.24}$$

Where

$$W_n = \sum_{n=1}^{\infty} 2\pi \frac{\bar{P}}{\bar{\alpha}_n^2} \left[1 + \frac{\bar{\alpha}_n \bar{H}(e^{2\bar{\alpha}_n \bar{H}} + 1)}{12\psi \left(\frac{h_0}{h} \right)^3 (e^{2\bar{\alpha}_n \bar{H}} - 1)} \right]^{-1}.$$

(6.25)

6.3 Numerical Calculations and Discussion of Results

It is clear from equations (6.22) and (6.24) that, the increase in dimensionless film pressure $\bar{p}$ and load-carrying capacity $\bar{W}$ is due to the first term on the right hand side, when FF is used as lubricant. Whereas the increase in $\bar{p}$ and $\bar{W}$ due to the terms P_n in equation (6.22) (defined in equation (6.23)) and W_n in equation (6.24) (defined in equation (6.25)) are because of the presence of the effect of pressure difference at the film-porous interface. It should be noted here that

$$P_n = f(P, h, a, H^*, h_0, \dot{h}, r, J_0, J_1, \phi, \eta, \alpha_n)$$

Thus, any change in any of the parameters of f will effect on P_n, and so its influence on the problem cannot be neglected. The similar argument can be made for $\bar{W}$.

The dimensionless film pressure $\bar{p}$ and load-carrying capacity $\bar{W}$ are numerically calculated and presented graphically for the following value of different parameters [21,23], which are remain fixed unless and until the calculation is made with respect to the variation of that particular parameter.

$$a = 0.05\,(\mathrm{m}), r = 0.025\,(\mathrm{m}), h_0 = 5.0\times10^{-5}\,(\mathrm{m}), h = 5.0\times10^{-6}\,(\mathrm{m})$$
$$\eta = 0.012\,(\mathrm{Ns\,m^{-2}}), \bar{\mu} = 0.05, \mu_0 = 4\pi\times10^{-7}\,(\mathrm{NA^{-2}}), P = 0.0001\,(\mathrm{Nm^{-2}})$$
$$K = 10^9 / 0.37\,(\mathrm{A^2 m^{-4}}), \dot{h} = -0.005\,(\mathrm{ms^{-1}}), \phi = 5.0\times10^{-14}\,(\mathrm{m^2}), H^* = 5.0\times10^{-5}\,(\mathrm{m}).$$

The calculation of magnetic field strength in order to make the required active contact zone in the neighbourhood of $r = 2a / 3$ is shown below: From equation (6.1)

$$\text{Max } \mathrm{H}^2 = 0.37 \times 10^{-3} \mathrm{K} \text{ for a} = 0.05$$

$$\text{For } K = 10^9 / 0.37,\ H = O(10^3)$$

Moreover, the formula for Bessel function of first kind of order zero and order one considered in the calculation [24,25] are respectively as follows.

$$J_0(x) = \frac{1}{6} + \left(\frac{1}{3}\right)\cos\left(\frac{x}{2}\right) + \left(\frac{1}{3}\right)\cos\left(\frac{\sqrt{3}x}{2}\right) + \left(\frac{1}{6}\right)\cos x,$$

$$J_1(x) = \left(\frac{1}{6}\right)\sin\left(\frac{x}{2}\right) + \left(\frac{1}{6}\right)\sin x + \left(\frac{\sqrt{3}}{6}\right)\sin\left(\frac{\sqrt{3}x}{2}\right).$$

Moreover, in equations (6.22) - (6.25) the summation extends for 10 terms.

Figure 6.2 shows variation in $\bar{p}$ as a function of dimensionless radial parameter R (where r varies). It is observed that $\bar{p}$ decreases rapidly with the increase of R. That means neighbourhood of the central area of the bearing bears greater load as compared to the area near the end of the bearing, which results in less wear. The variation in $\bar{p}$ and $\bar{W}$ with respect to dimensionless minimum film thickness parameter (h_0/h) (where h varies) is shown in Figure 6.3 and Figure 6.4, respectively. It is observed that with the increase of (h_0/h), $\bar{p}$ and $\bar{W}$ decreases. That means for larger value of minimum film thickness (h), $\bar{p}$ and $\bar{W}$ increases. This may be because of the generation of stronger and nearer to fully developed FF spikes (which is due to the effect of magnetic field) for values of $(h_0 / h) \le 10$; that is; for larger value of minimum film thickness. Moreover, it can also be seen from Figure 6.4 that $\bar{W}$ decreases moderately with the increase of (h_0/h). That

means even though rapid decrease in $\bar{p}$, the load-carrying capacity $\bar{W}$ maintained well. Figures 6.5 and 6.6 shows respectively the variation in $\bar{p}$ and $\bar{W}$ as a function of dimensionless magnetization parameter μ^* (where K varies). It is observed that $\bar{p}$ and $\bar{W}$ remains same up to $\mu^* = 3.54\times10^{-2}$, but beyond that it increases. That means both $\bar{p}$ and $\bar{W}$ increases with the increasing values of magnetic field strength. This may be because of increasing strongest nature of the generated spikes. Moreover, it can also be seen from both the figures that $\bar{W}$ increase proportionally with $\bar{p}$.

6.4 Conclusions

Modified Reynolds equation is derived for FF lubricated squeeze-film bearing made by flat circular porous upper and impermeable lower discs. The equations from ferrohydrodynamics theory by R.E. Rosensweig and equation of continuity for film as well as porous region are used in the derivation under the assumption of validity of Darcy's law in the porous region. In order to control FF, oblique VMF is used. The VMF is considered because uniform magnetic field does not enhance bearing performances (refer equation (6.3)). Moreover, it is important because of its advantage of generating maximum field at the required active contact zone. In the present analysis the active contact zone is considered at the middle of the lower disc and so the applied magnetic field is chosen to be maximum at that point. Expression for film pressure is obtained in terms of Bessel function by considering the effect of existence of pressure difference at the film-porous interface. The effect of existence of pressure difference is considered because it violets the assumptions of Morgan-Cameron approximation and continuity of the pressure at the film-porous interface. The effects of dimensionless radial parameter,

minimum film thickness parameter and magnetization parameter are studied on $\bar{p}$, whereas the effects of minimum film thickness parameter and magnetization parameter are studied on $\bar{W}$. The Results show that $\bar{p}$ increases for smaller values of radial parameter, larger values of magnetization parameter and when $(h_0 / h) \leq 10$, whereas $\bar{W}$ increases for larger values of magnetization parameter and when $(h_0 / h) \leq 10$.

6.5 Figures

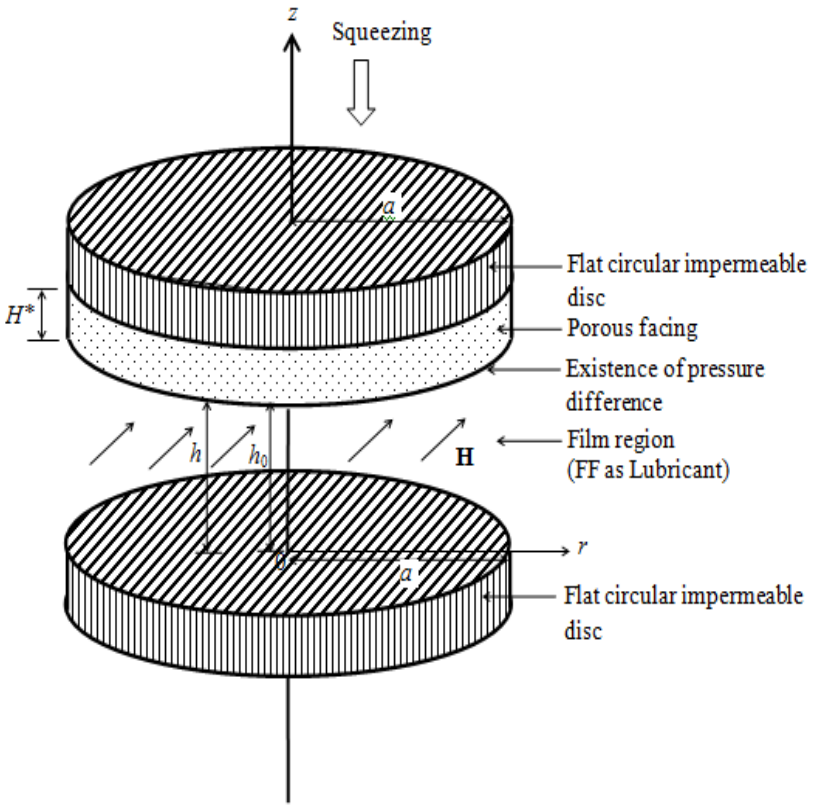

Figure 6.1

Schematic diagram of squeeze-film bearing made by flat circular porous upper and impermeable lower discs.

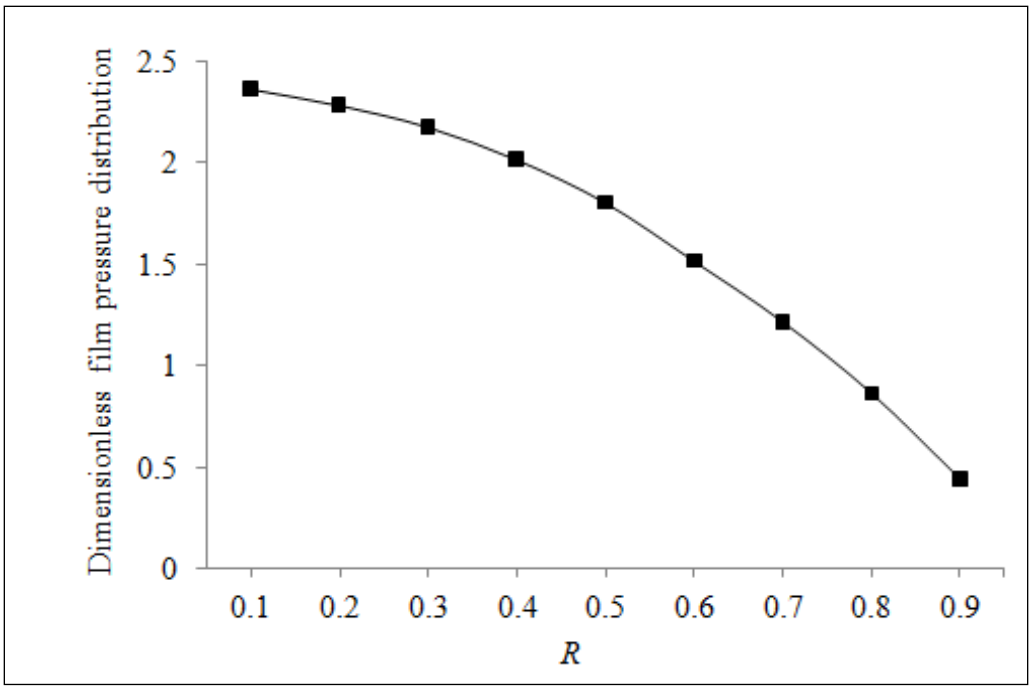

Figure 6.2

Variation in dimensionless film pressure $\bar{p}$ for different values of dimensionless radial parameter R

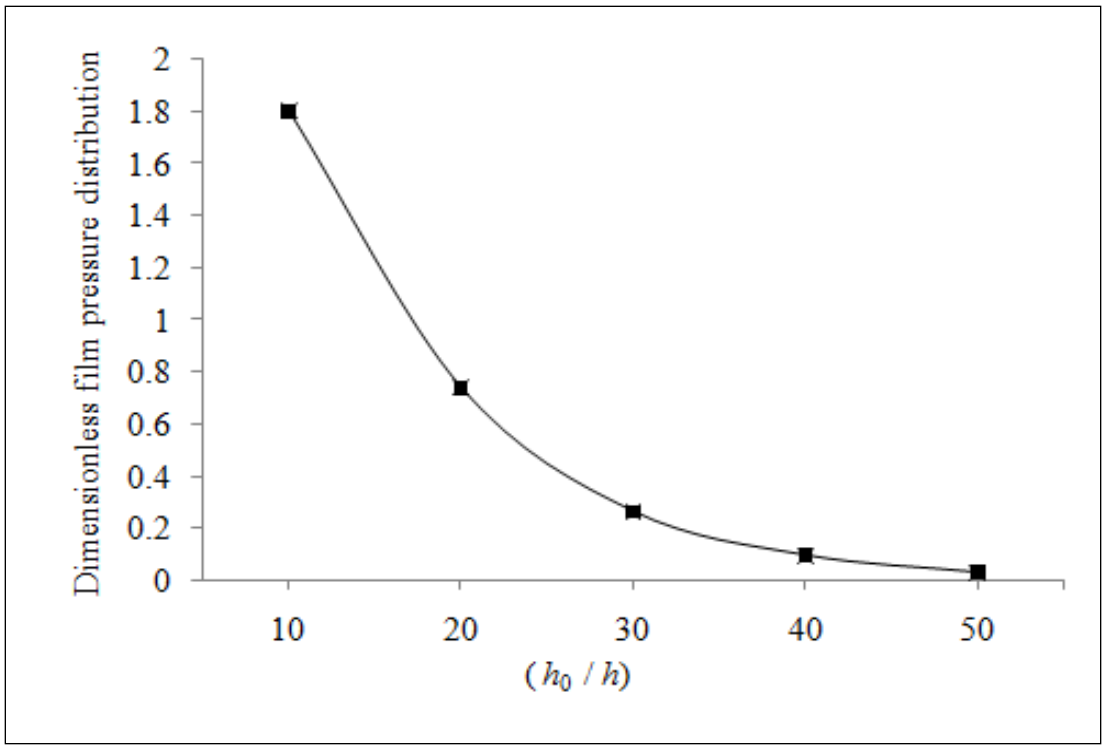

Figure 6.3

Variation in dimensionless film pressure $\bar{p}$ for different values of dimensionless minimum film thickness parameter (h_0/h)

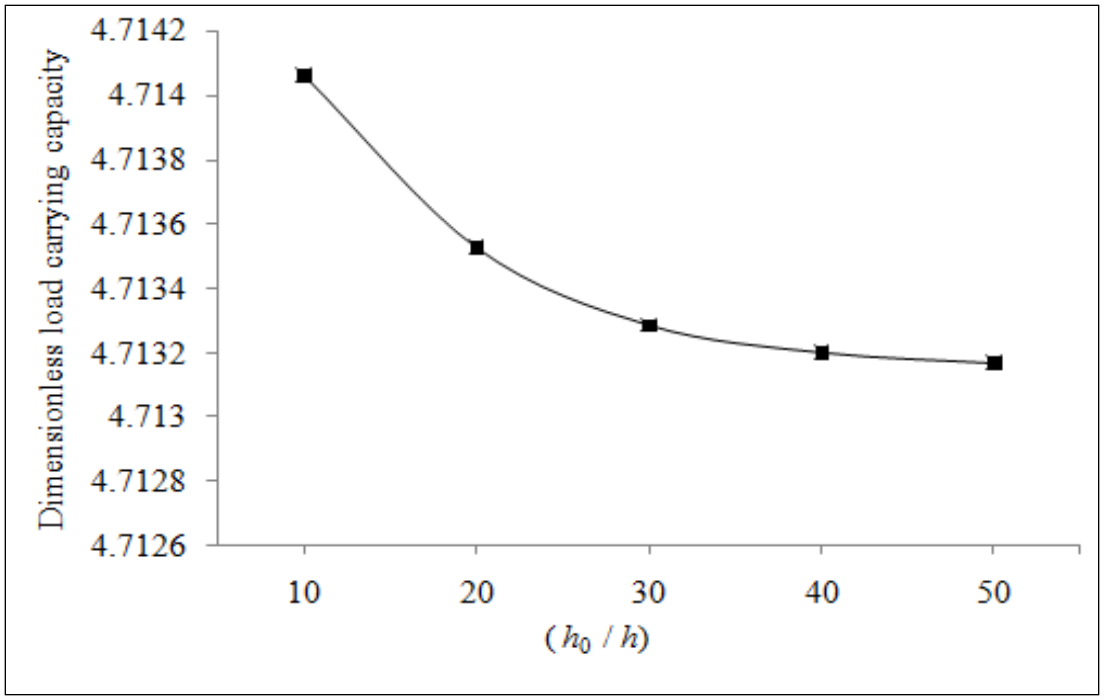

Figure 6.4

Variation in dimensionless load-carrying capacity $\bar{W}$ for different values of dimensionless minimum film thickness parameter (h_0/h)

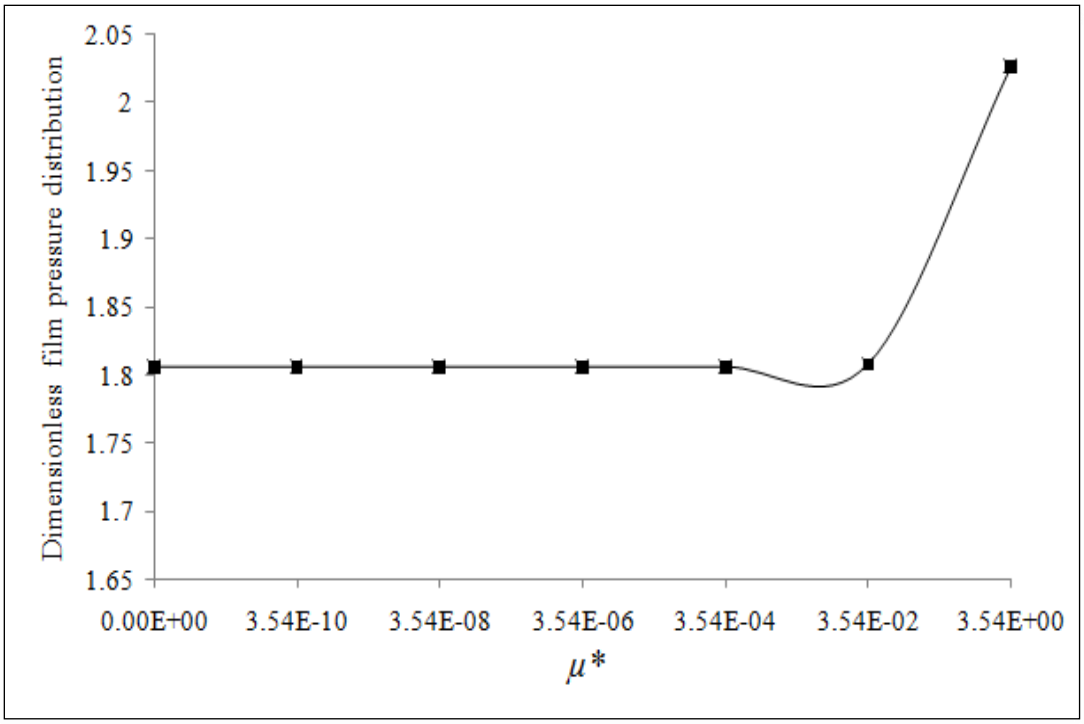

Figure 6.5

Variation in dimensionless film pressure $\bar{p}$ for different values of dimensionless magnetization parameter μ^*

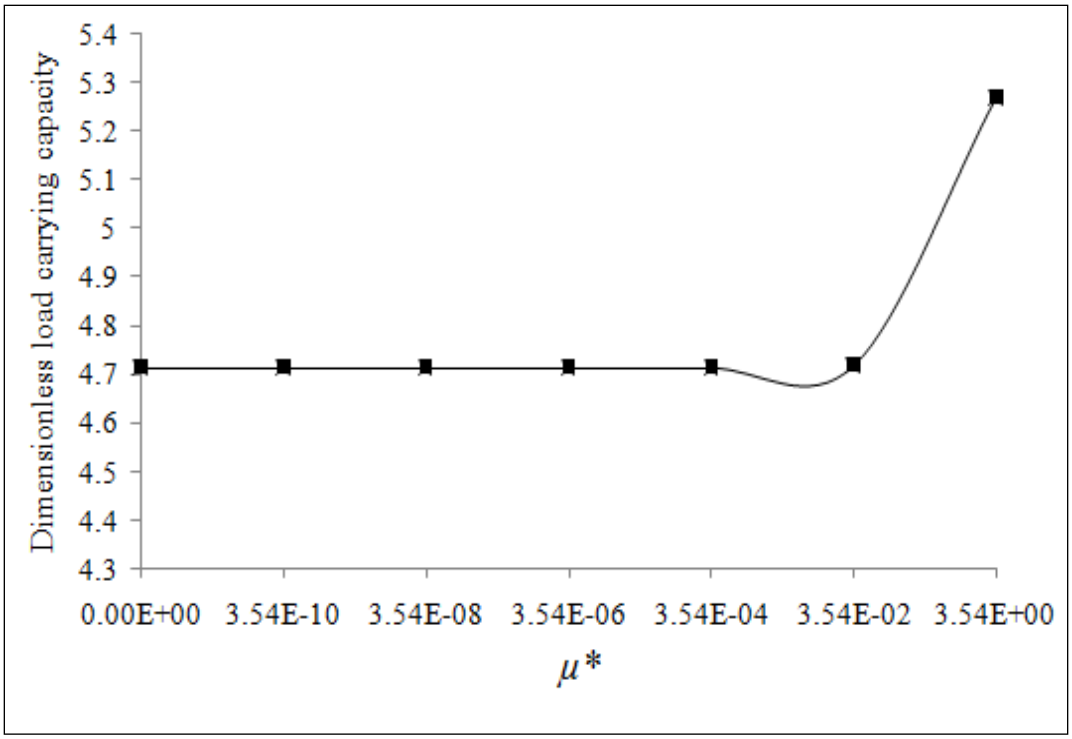

Figure 6.6.

Variation in dimensionless load-carrying capacity $\bar{W}$ for different values of dimensionless magnetization parameter μ^*

6.6 References

[1] H. Wu, Squeeze-film behaviour for porous annular disks, *Journal of Lubrication Technology* 92(4) (1970) 593-596.

[2] E.M. Sparrow, G.S. Beavers and I.T. Hwang, Effect of velocity slip on porous–walled squeeze-films, *Journal of Lubrication Technology* 94 (1972) 260-265.

[3] P.R.K. Murti, Squeeze-film behaviour in porous circular disks, *Journal of Lubrication Technology* 96 (1974) 206-209.

[4] J.L. Gupta and K.C. Patel, Effect of axial pinch on the porous walled squeeze-film with velocity slip, *Wear* 31 (1975) 381-389.

[5] J.L. Gupta, K.H. Vora and M.V. Bhat, The effect of rotational inertia on the squeeze-film load between porous annular curved plates, *Wear* 79 (1982) 235-240.

[6] J. Prakash and K. Tiwari, Effect of surface roughness on the squeeze-film between rotating porous annular discs with arbitrary porous wall thickness, *International Journal of Mechanical Sciences* 27(3) (1985) 135-144.

[7] M.V. Bhat and G.M. Deheri, Magnetic-fluid-based squeeze-film in curved porous circular discs, *Journal of Magnetism and Magnetic Materials* 127 (1993) 159-162.

[8] A.A. Elsharkawy and M.M. Nassar, Hydrodynamic lubrication of squeeze-film porous bearings, *Acta Mechanica* 118 (1996) 121-134.

[9] R.C. Shah and M.V. Bhat, Squeeze-film based on magnetic fluid in curved porous rotating circular plates, *Journal of Magnetism and Magnetic Materials* 208 (2000) 115-119.

[10] R.C. Shah and M.V. Bhat, Combined effect of anisotropic permeability and slip velocity on porous-walled squeeze-films lubricated with a ferrofluid, *Journal of Friction and Wear* 24(1) (2003) 58-64.

[11] A. Walicka, E. Walicki, P. Jurczak and D. Michalski, Inertia effects in a curvilinear squeeze-film bearing with one porous wall lubricated by a power–law fluid, *International Journal of Applied Mechanics and Engineering* 8(1) (2003) 107-116.

[12] R.C. Shah and M.V. Bhat, Ferrofluid lubrication of a parallel plate squeeze film bearing, *Theoretical and Applied Mechanics* 30(3) (2003)) 221-240.

[13] R.C. Shah and M.V. Bhat, Anisotropic permeable porous facing and slip velocity on squeeze-film in an axially undefined journal bearing with ferrofluid lubricant, *Journal of Magnetism and Magnetic Materials* 279 (2004) 224-230.

[14] G.M. Deheri and R.M. Patel, Squeeze-film based magnetic fluid in between porous circular disks with sealed boundary, *International Journal of Applied Mechanics and Engineering* 11(4) (2006) 803-812.

[15] R.C. Shah and M.V. Bhat, Ferrofluid-lubricated secant-shaped squeeze-film bearing with anisotropic permeability, slip-velocity, material parameter and rotational inertia, *FIZIKA A* 16(4) (2007) 167-178.

[16] N.M. Bujurke, D.P Basti and R.B. Kudenatti, Surface roughness effects on squeeze-film behaviour in porous circular disks with couple-stress fluid, *Transp. Porous. Med.* 71 (2008) 185-197.

[17] M. Rajashekar and B. Kashinath, Effect of surface roughness on MHD couple-stress squeeze-film characteristics between a sphere and a porous plane surface, *Advances in Tribology* (2012) Article ID 935690, 10 pages, doi: 10.1155/2012/935690.

[18] R.C. Shah and D.B. Patel, Squeeze-film based on ferrofluid in curved porous circular plates with various porous structure, *Applied Mathematics* 2(4) (2012) 121-123.

[19] S.T. Fathima, N.B. Naduvinamani, S.H. Marulappa and H. Bannihalli, A study on the performance of hydromagnetic squeeze-film between anisotropic porous rectangular plates with couple-stress fluids, *Tribology Online* 9(1) (2014) 1-9.

[20] R.C. Shah, N.I. Patel and R.C. Kataria, Some porous squeeze-film-bearings using ferrofluid lubricant: A review with contributions, *Institution of Mechanical Engineers, Part J: Journal of Engineering Tribology* 230(9) (2016) 1157-1171.

[21] R.C. Shah and R.C. Kataria, On the squeeze-film characteristics between a sphere and a flat porous plate using ferrofluid, *Applied Mathematical Modelling* 40 (2016) 2473-2484.

[22] R.E. Rosensweig, Ferrohydrodynamics, *Cambridge University Press*, York (1985).

[23] M.M. Khonsari and E.R. Booser, Applied Tribology: Bearing design and lubrication, *John Wiley & Sons Inc*. (2001).

[24] M.T. Abuelma'Atti, Trigonometric Approximations for some Bessel Functions, *Active and Passive Elec. Comp.* 22 (1999) 75-85.

[25] R.C. Shah, Differential equations, *Books India Publications*, Gujarat, India (2012).